46. Cyclization of Hydroxyenol Ethers into Spiroacetals. Evidence for the Position of the Transition State and Its Implication on the Stereoelectronic Effects in Acetal Formation

by **Normand Pothier, Solo Goldstein,** and **Pierre Deslongchamps***

Laboratoire de synthèse organique, Département de chimie, Faculté des sciences, Université de Sherbrooke, Sherbrooke, Québec, Canada J1K 2R1

(14.XI.91)

Acid-catalyzed cyclizations under thermodynamically and kinetically controlled conditions of the hydroxyenol ethers **18**–**21** are reported. Thermodynamically controlled cyclizations of **18**, **19**, and **21** produced only the more stable corresponding spiroacetals **22** and **27**. Thermodynamically controlled cyclization of compound **20** produced a 1:1 mixture of non-epimerisable spiroacetals **24** and **26**. On the other hand, kinetically controlled cyclizations of the same four hydroxyenol ethers produced, along with the more stable spiroacetals mentioned above, the less stable spiroacctals **23**, **25**, and **28**. These results show that the kinetically controlled cyclization takes place *via* an early transition state which produces a mixture of the less stable and the more stable isomers. These results are explained by an early transition state taking into account the principle of stereoelectronic control while following the antiperiplanar lone-pair hypothesis (*Bürgi-Dunitz* angle of attack of a nucleophile on a π system).

Introduction. – We previously reported [1] a study which revealed that the unsubstituted 1,7-dioxaspiro[5.5]undecane exists exclusively in conformation $\mathbf{A}_1$ (*Scheme 1*), even at room temperature. This experimental observation was explained by the fact that conformation $\mathbf{A}_1$ is stereoelectronically and sterically more stable than conformations $\mathbf{A}_2$ and $\mathbf{A}_3$ which were estimated to be less stable by a value of 2.4 and 4.8 kcal/mol, respectively[1]). This result was further confirmed experimentally by comparing the behavior of 1-oxaspiro[5.5]undecane which was shown to exist as an equilibrium mixture of two conformers [2].

Scheme 1

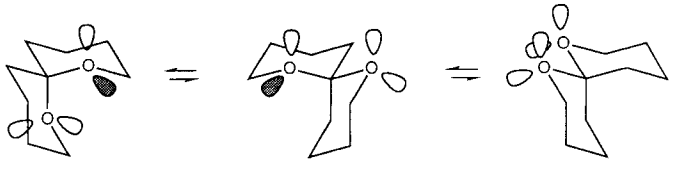

$\mathbf{A}_1$ (0) $\mathbf{A}_2$ (2.4 kcal/mol) $\mathbf{A}_3$ (4.8 kcal/mol)

[1]) The relative energy of 0, 2.4, and 4.8 kcal/mol for $\mathbf{A}_1$, $\mathbf{A}_2$, and $\mathbf{A}_3$ was estimated by using the following values: anomeric effect (e) = −1.4 kcal/mol; steric effect: *gauche* form of butane (CC) = 0.9 kcal/mol, *gauche* (synclinal) form of CH_2–CH_2–CH_2–O (CO) = 0.4 kcal/mol, and *gauche* form of CH_2–O–CH_2–O (CO) = 0.4 kcal/mol. Conformer $\mathbf{A}_1$, $2e + 4\ CO = -1.2$ kcal/mol, conformer $\mathbf{A}_2$, $1e + 2\ CC + 2\ CO = 1.2$ kcal/mol, and conformer $\mathbf{A}_3$, $4\ CC = 3.6$ kcal/mol.

We also showed [1] that the thermodynamically controlled formation of substituted 1,7-dioxaspiro[5.5]undecanes obtained by acid cyclization of the corresponding dihydroxyketo precursors produced only the isomer having a conformation corresponding of that of $\mathbf{A}_1$. *E.g.*, 2-methyl-1,7-dioxaspiro[5.5]undecane was formed as isomer **22** (see below), none of isomer **23** which corresponds to conformation $\mathbf{A}_2$ being observed. Similarly, the tricyclic spiroacetal isomer **27** was produced exclusively under similar conditions, none of isomer **28** being formed.

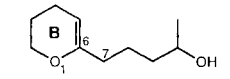

18 (arbitrary numbering)

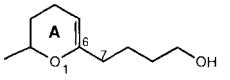

19

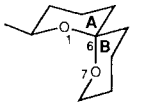

22 (0 kcal/mol)
(systematic numbering)

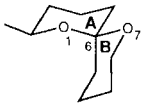

23 (2.4 kcal/mol)

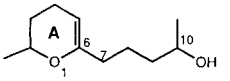

20

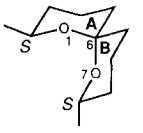

24 (0 kcal/mol)

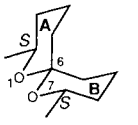

25 (4.8 kcal/mol)

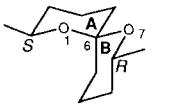

26 (2.4 kcal/mol)

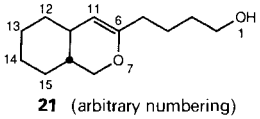

21 (arbitrary numbering)

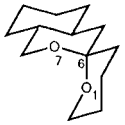

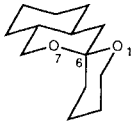

27 (0 kcal/mol)
(arbitrary numbering)

28 (2.4 kcal/mol)

We wish now to report the *kinetically* and *thermodynamically controlled* formation of three sets of spiroacetals from the cyclization of hydroxyenol ethers **18–21** under acid conditions. As will be shown, this work provides experimental evidence for the position of the transition state along the reaction coordinate of the cyclization process. As a result, this new knowledge might be used to gain a better understanding of stereoelectronic [3] [4] and steric factors controlling the general mechanism of acetal formation or hydrolysis.

Results. – *Synthesis.* Hydroxyenol ethers **18–21** were prepared as follows. The lithium acetylide derivative of acetylenic silyl ether **4** or **5** (BuLi/THF) was reacted with the appropriate lactone **1**, **2**, or **3** to give the corresponding ynones **6–9** which were hydrogenated (H_2/PtO_2) to give the hydroxyketones **10–13**. Elimination of H_2O (TsOH/benzene) produced the silylated intermediates **14–17** which were converted ($(Bu)_4NF$/THF) into the four desired hydroxyenol ethers **18–21**.

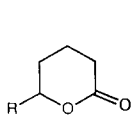

1 R = H
2 R = CH_3

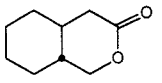

3

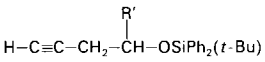

4 R′ = H
5 R′ = CH_3

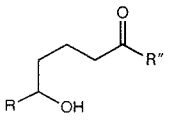

6 R = H, R″ = C≡CCH_2CH(Me)$OSiPh_2$(*t*-Bu)
7 R = Me, R″ = C≡$CCH_2CH_2OSiPh_2$(*t*-Bu)
8 R = Me, R″ = C≡CCH_2CH(Me)$OSiPh_2$(*t*-Bu)
10 R = H, R″ = $(CH_2)_3CH$(Me)$OSiPh_2$(*t*-Bu)
11 R = Me, R″ = $(CH_2)_4OSiPh_2$(*t*-Bu)
12 R = Me, R″ = $(CH_2)_3CH$(Me)$OSiPh_2$(*t*-Bu)

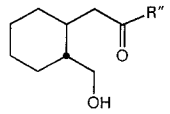

9 R″ = C≡$CCH_2CH_2OSiPh_2$(*t*-Bu)
13 R″ = $(CH_2)_4OSiPh_2$(*t*-Bu)

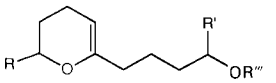

14 R = H, R′ = Me, R‴ = (*t*-Bu)Ph_2Si
15 R = Me, R′ = H, R‴ = (*t*-Bu)Ph_2Si
16 R = Me, R′ = Me, R‴ = (*t*-Bu)Ph_2Si
18 R = H, R′ = Me, R‴ = H
19 R = Me, R′ = H, R‴ = H
20 R = Me, R′ = Me, R‴ = H

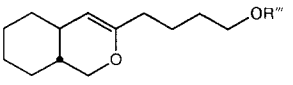

17 R‴ = (*t*-Bu)Ph_2Si
21 R‴ = H

Cyclizations under Kinetic and Thermodynamic Control. Cyclization experiments of hydroxyenol ethers **18–21** were carried out with AcOH in benzene (kinetic control) and with CF_3COOH in benzene (thermodynamic control). C_6D_6 was used as solvent in all experiments which were carried out in an NMR tube, and ^{13}C-NMR was used to analyze product formation. The ^{13}C-NMR data for the four hydroxyenol ethers **18–21** and the corresponding spiroacetals **22–28** are reported in *Table 1*. The relative configuration of spiroacetals **22–28** was established from their ^{13}C-NMR data using the well known semiempirical derivation of ^{13}C-NMR chemical shifts [5] and by comparison with the already known corresponding spiroacetals [1].

Table 1. *^{13}C-NMR Chemical Shift Data for Compounds* **18–28**. δ in ppm rel to TMS; at 300 K in C_6D_6.

	C(2)	C(3)	C(4)	C(5)	C(6)	C(7)	C(8)	C(9)	C(10)	Me–C(2)	*Me*–C(10) or *Me*–C(8)
18[a])	66.0 (*t*)	22.8 (*t*)	20.6 (*t*)	95.2 (*d*)	154.9 (*s*)	34.8 (*t*)	23.7 (*t*)	39.1 (*t*)	67.5 (*d*)	23.7 (*q*)	
19[a])	71.5 (*d*)	29.6 (*t*)	20.8 (*t*)	94.7 (*d*)	154.6 (*s*)	34.5 (*t*)	23.8 (*t*)	32.6 (*t*)	62.4 (*t*)	21.2 (*q*)	
20[a])	71.5 (*d*)	29.6 (*t*)	20.8 (*t*)	94.6 (*d*)	154.6 (*s*)	34.7 (*t*)	23.7 (*t*)	39.2 (*t*)	67.6 (*d*)	21.2 (*q*)	23.7 (*q*)
22	65.2 (*d*)	33.1 (*t*)	19.4 (*t*)	35.6 (*t*)	95.5 (*s*)	–	60.1 (*t*)	25.8(*t*)	19.0 (*t*)	36.2 (*t*)	22.1 (*q*)
23	68.4 (*d*)	32.5 (*t*)	19.0 (*t*)	36.3 (*t*)	96.4 (*s*)	–	61.0 (*t*)	26.1 (*t*)	18.8 (*t*)	30.9 (*t*)	22.1 (*q*)
24	65.1 (*d*)	33.2 (*t*)	19.3 (*t*)	35.6 (*t*)	96.1 (s)	–	65.1 (*d*)	33.2 (*t*)	19.3 (*t*)	35.6 (*t*)	22.2 (*q*) 22.2 (*q*)
25	68.5 (*d*)	32.3 (*t*)	19.4 (*t*)	30.9 (*t*)	98.7 (*s*)	–	68.5 (*d*)	32.3 (*t*)	19.4 (*t*)	30.9 (*t*)	22.8 (*q*) 22.8 (*q*)
26	68.5 (*d*)	32.6 (*t*)	19.1 (*t*)	36.6 (*t*)	97.1 (*s*)	–	65.9 (*d*)	33.5 (*t*)	19.2 (*t*)	30.3 (*t*)	22.3 (*q*) 22.1 (*q*)

	C(2)	C(3)	C(4)	C(5)	C(6)	C(7)	C(8)	C(9)	C(10)	C(11)	C(12)	C(13)	C(14)	C(15)
21[b])	62.5 (*t*)	32.6 (*t*)	23.8 (*t*)	34.2 (*t*)	153.7 (*s*)		71.1(*t*)	39.7 (*d*)	38.6 (*d*)	100.4 (*d*)	33.0 (*t*)	26.6 (*t*)	26.5 (*t*)	28.1 (*t*)
27[c])	60.3 (*t*)	25.7 (*t*)	18.7 (*t*)	35.8 (*t*)	96.2 (*s*)	–	65.4 (*t*)	41.8 (*d*)	35.6 (*d*)	43.5 (*t*)	33.1 (*t*)	26.3 (*t*)	26.6 (*t*)	27.9 (*t*)
28[c])	61.5 (*t*)	25.8 (*t*)	19.0 (*t*)	35.9 (*t*)	97.5 (*s*)	–	68.0 (*t*)	42.0 (*d*)	37.1 (*d*)	44.1 (*t*)	33.3 (*t*)	26.1 (*t*)	26.4 (*t*)	28.1 (*t*)

[a]) Arbitrary numbering, see *Formula* **18**.
[b]) Arbitrary numbering, see *Formula* **21**.
[c]) Arbitrary numbering, see *Formula* **27**.

Cyclization of hydroxyenol ether **18** with CF_3COOH/benzene was complete within 2 h and gave the known spiroacetal **22** [1] in quantitative yield. On the other hand, treatment of **18** with AcOH/benzene during 19 h gave a 1:1 mixture of spiroacetals **22** and **23**. This ratio was shown to remain unchanged under these mild acidic conditions. It was also observed that the mixture **22** and **23** was equilibrated (< 2 h) upon treatment with CF_3COOH/benzene to give only spiroacetal **22**. These results show rigorously that AcOH/benzene and CF_3COOH/benzene provide conditions for a kinetically and thermodynamically controlled cyclization, respectively. Repeating similar experiments with hydroxyenol ether **19** under thermodynamic control (CF_3COOH/benzene, 2 h) gave again only spiroacetal **22** and under kinetic control (AcOH/benzene, 19 h) **22**/**23** in a 3:2 ratio.

Analogous results were obtained with bicyclic hydroxy-enol ether **21**. Under thermodynamic control (CF_3COOH/benzene, 2 h), the known [1] tricyclic spiroacetal **27** was formed exclusively, whereas under kinetic control (AcOH/benzene, 10 h), a 3:2 ratio of isomeric spiroacetals **27** and **28** was observed. Again, upon treatment with CF_3COOH/benzene (< 2 h), the mixture **27**/**28** underwent equilibration to give only spiroacetal **27**.

The cyclization of hydroxyenol ether **20** which is a 1:1 mixture of diastereoisomeric racemic pairs ((2*RS*,2′*SR*) and (2*RS*,2′*RS*)) due to the presence of the two secondary methyl groups, was next examined. Cyclization of the diastereoisomeric mixture **20** with CF_3COOH/benzene gave a 1:1 mixture of spiroacetals **24** and **26**. On the other hand, cyclization of **20** with AcOH/benzene provided a mixture of three spiroacetals **24**, **25**, and **26** in a relative ratio of 3:2:5. Upon treatment with CF_3COOH/benzene, this mixture was converted into a mixture **24**/**26** in a 1:1 ratio.

Discussion. – As previously discussed, a spiroacetal exists in conformation $\mathbf{A}_1$ unless there is a severe 1,3-diaxial steric interaction between the substituents and the ring skeletons. In such a case, the compound will normally adopt conformation $\mathbf{A}_2$, unless there is again severe 1,3-diaxial steric interaction which will force the compound to adopt conformation $\mathbf{A}_3$.

Conformational analysis of substituted spiroacetals **22**, **23**, **27**, and **28** was discussed in detail previously [1]. Compounds **22** and **27** were shown to exist in conformation $\mathbf{A}_1$, and it was predicted that compounds **23** and **28** exist in conformation $\mathbf{A}_2$. Also, the relative stability of isomers **22** and **23** which can be interconverted by acid isomerization was estimated to be 0 and 2.4 kcal/mol, respectively. Similarly, isomer **28** was estimated to be 2.4 kcal/mol less stable than isomer **27**.

The conformational analysis of dimethyl spiroacetals **24**–**26** was not reported previously. Isomer **24** can take theoretically three different conformations corresponding to $\mathbf{A}_1$, $\mathbf{A}_2$, and $\mathbf{A}_3$, but using the previously described parameters [1], it can be predicted that the $\mathbf{A}_1$-like conformation will be more stable as shown in *Scheme 2*. Isomer **25** can also take three different conformations (corresponding to $\mathbf{A}_1$, $\mathbf{A}_2$, and $\mathbf{A}_3$), and the most stable one is predicted to correspond to $\mathbf{A}_3$. The relative stability of isomers **24** and **25** which can be interconverted under acidic conditions can also be estimated to be 0 and 4.8 kcal/mol by comparing their most stable conformation. Finally, isomer **26** which cannot be interconverted by acid isomerization to isomers **24** and **25** can theoretically adopt 4 different conformations (corresponding to $\mathbf{A}_1$, $\mathbf{A}_3$, and $\mathbf{A}_2$ (2 conformations)) but the $\mathbf{A}_2$-like conformation with two equatorial Me groups is predicted to be the most stable conformation.

Scheme 2. *Conformational Analysis of Spiroacetals* **24–26**

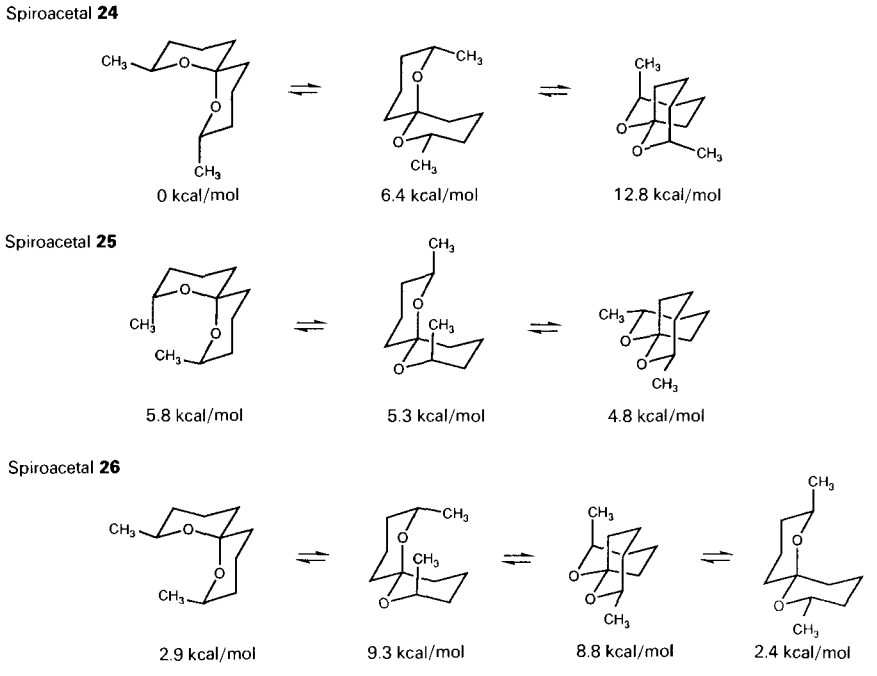

The results obtained under thermodynamically controlled conditions can be easily rationalized because we can evaluate the relative energy of the various possible conformations of the spiroacetal isomers, as well as the relative stability of the spiroacetal isomers which can be interconverted under acid conditions. Thus, since isomer **23** is 2.4 kcal/mol less stable than isomer **22**, the exclusive formation of **22** when the cyclization is carried out with CF_3COOH/benzene (thermodynamic control) is readily understood. Similarly, only isomer **27** was observed in the cyclization of **21** under thermodynamic control, because **27** is more stable (2.4 kcal/mol) than isomer **28**. The (2*RS*,2′*RS*)-diastereoisomer of hydroxyenol ether **20** can give racemic spiroacetals **24** and **25**, whereas the (2*RS*,2′*SR*)-diastereoisomer can only lead to racemic spiroacetal **26**. However, since we know that **24** and **25** are interconvertible under acid conditions (but not **26**) and that **25** is estimated to be less stable than **24** by 4.8 kcal/mol, it follows that the cyclization of the (racemic) diastereoisomer mixture **20** under thermodynamic control should lead to a 1:1 mixture of **24** and **26**, in complete agreement with the experimental results.

It remains to explain the results obtained in the cyclizations under kinetic control. Under such conditions, the reaction products are independent of their relative stability, but rather depend upon the relative energy of the transition states leading to them.

It is reasonable to assume that on cyclization **18** will be protonated [6] [7] to give an oxocarbonium ion which can exist in two rapidly equilibrating conformations **29a** and **29b** (*Scheme 3*). This would then be followed by a stereoelectronically controlled reaction assuming an antiperiplanar attack [3]. Thus, an α-attack on conformation **29a** (→**32**→**33**) and a β-attack on conformation **29b** (→**34**→**35**) lead to chair-like transition

states, while a β-attack on **29a** (→**30**→**31**) and an α-attack on **29b** (→**36**→**37**) lead to twist-boat transition states. If it is assumed that transition states are late, resembling the protonated spiroacetals, the sterically disfavored twist-boats **31** and **37** are eliminated, and it appears possible to explain the observed 1:1 ratio of **22** and **23** by the chair-like transition states. Indeed, stereoelectronic effects are equivalent and steric effects are relatively similar in **32**→**33** and **34**→**35**, especially if it is considered that the formation of the C–O bond is not yet completed at the transition state. If it is assumed, however, that the transition state is very early, resembling **30**, **32**, **34**, and **36**, steric effects appear to be close in all cases, and the observed 1:1 ratio of **22** and **23** could be explained on that basis as well. Thus, the experimental results described so far cannot distinguish between an early or a late transition state.

Scheme 3

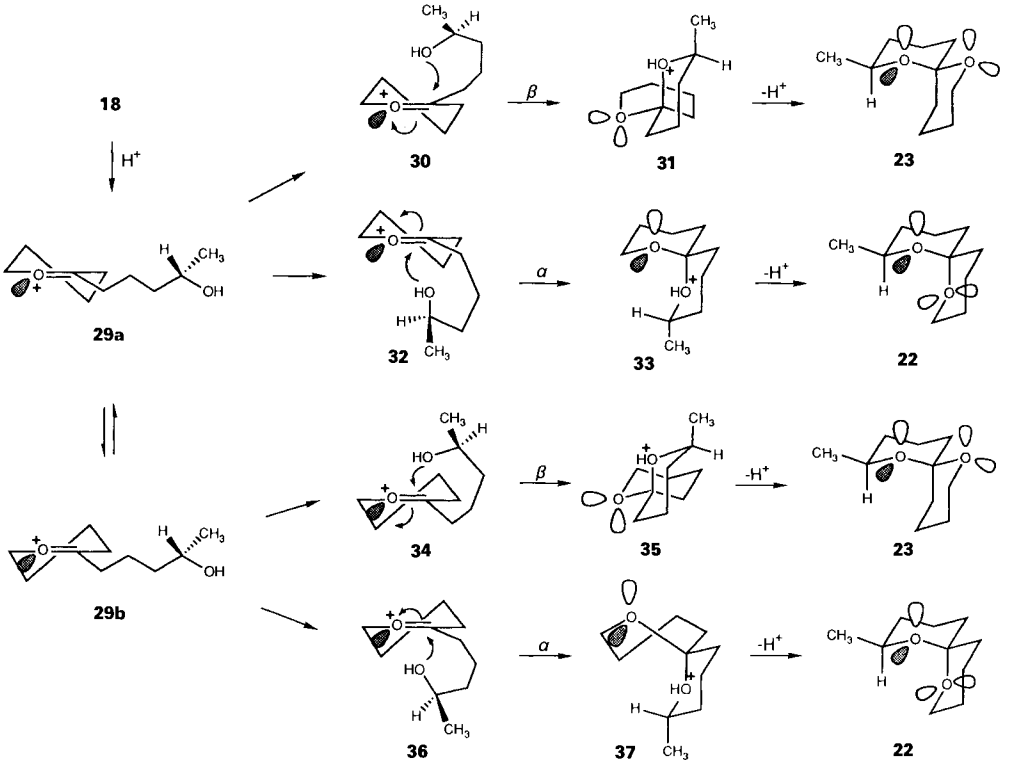

Under kinetic control of the cyclization of hydroxyenol ether **19** (→**22**/**23** 3:2), protonation will first produce an oxocarbonium ion which can have conformation **38a** or **38b**, the former being more stable (pseudoequatorial Me group) than the latter (*Scheme 4*). Again four possible modes of cyclization lead to two chair-like (→**41**→**42** and →**43**→**44**) and two twist-boat-like (→**39**→**40** and →**45**→**46**) transition states. The first chair-like transition state (**41**→**42**) should produce (after H^+ loss) the more stable spiroacetal **22**, whereas the second one (**43**→**44**) should give (after H^+ loss and conformational inversion of both rings) the less stable **23**. Process **41**→**42** is essentially devoid of severe

steric interactions, but **43**→**44** is severely hindered since the Me group in **44** is in a 1,3-diaxial orientation with the protonated O-atom. The two pathways leading to the twist-boat intermediates, *i.e.* **39**→**40** and **45**→**46**, are stereoelectronically equivalent (they are mirror images), except for the fact that the Me group is in a pseudoequatorial orientation in the process **39**→**40** and in a pseudoaxial orientation in the process **45**→**46**. Assuming now a late transition state, the two twist-boat-like transition states **40** and **46** are readily eliminated as well as the chair-like transition state **44** which experiences a severe 1,3-diaxial steric interaction. Thus, only spiroacetal **22** should have been produced (*via* **41**→**42**) which is in contrast to the experimental result. The assumption of an early transition state disfavors the two pathways involving oxocarbonium ion **38b** which is sterically less favored than **38a**. Furthermore, pathway **43**→**44** must experience some steric hindrance between the pseudoaxial Me group and the incoming OH group. On the other hand, both processes taking place on **38a** are relatively sterically free. It is, therefore, possible that the cyclization would take place only *via* **38a** where the chair-like process **41**→**42** would be very slightly favored over the twist-boat process **39**→**40** because of the very early nature of the transition state; this would explain the observed 3:2 ratio of **22**/**23**.

Scheme 4

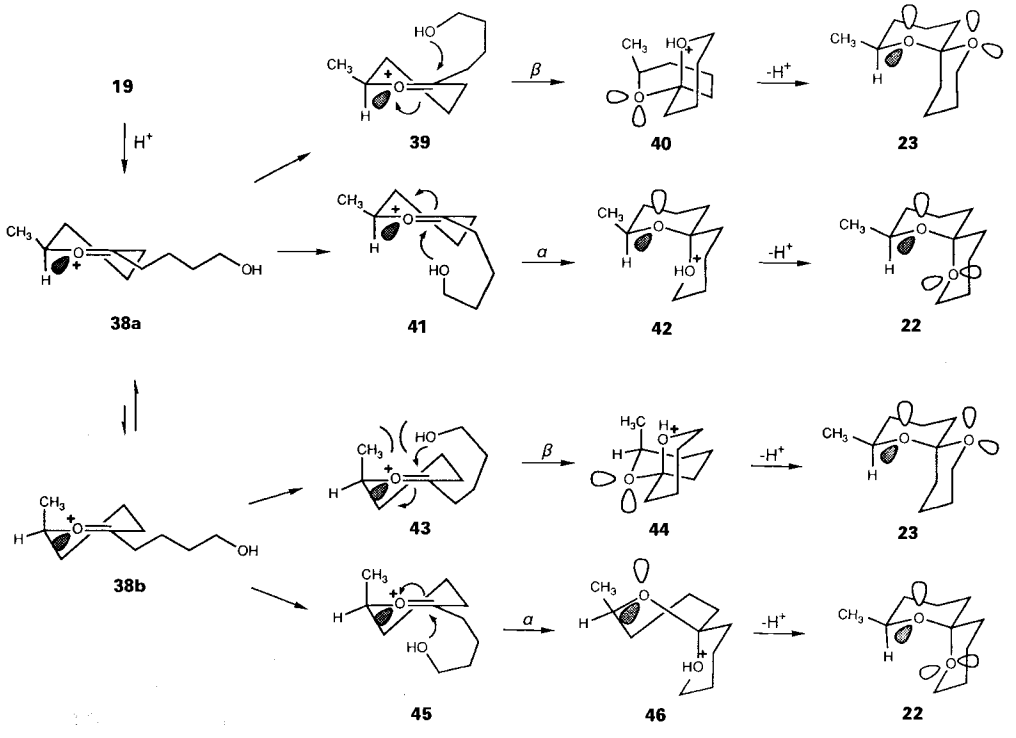

Examination of the results obtained with bicyclic hydroxyenol ether **21** under kinetic control (→**27**/**28** 3:2) confirms this conclusion. Protonation of **21** produces oxocarbonium ion **47** (*Schema 5*) which has a conformation **47a** essentially identical to that of **38a**

(or **29a**) but with the difference that ring inversion is no more possible due to the *trans*-junction of the bicyclic skeleton. Therefore, only two modes of attack which respect to the antiperiplanar hypothesis are left, the one *via* a twist-boat process (→**48**→**49**) to give the less stable spiroacetal **28** and one *via* a chair-like process (→**50**→**51**) to give the more stable spiroacetal **27**. Again, a late transition state cannot explain the experimental results since a geometry close to **49** is energetically too high by comparison with **51**. On the other hand, an early transition state can explain the fact that **48** (beginning of a twist-boat) should be slightly higher in energy then **50**, which is consistent with the observed 3:2 ratios of **27**/**28**.

Scheme 5

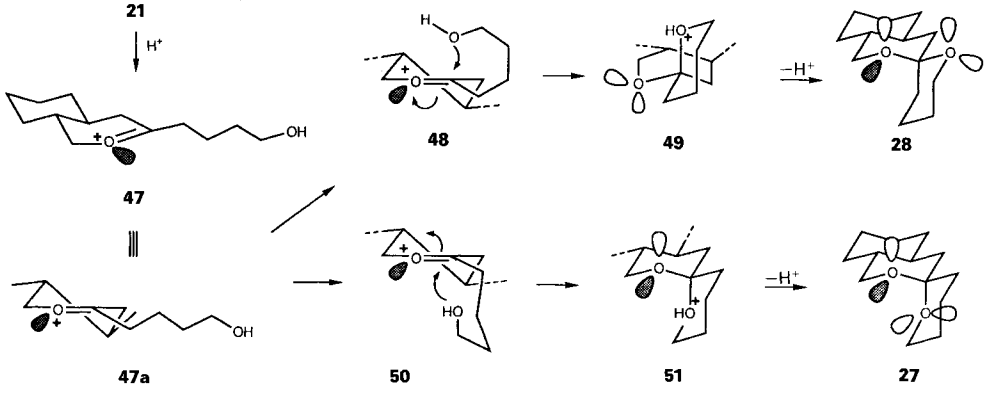

Since the 3:2 product ratio is the same for the cyclization under kinetic control of hydroxyenol ethers **19** and **21**, it can be concluded that the cyclization of oxocarbonium ion **38** probably takes place only from the ion **38a** (*via* **39**→**40**→**23** and **41**→**42**→**22** in a 2:3 ratio). In the case of hydroxyenol ether **18** which produce an oxocarbonium ion **29** which can exist in two energetically equivalent conformations (**29a** and **29b**), it can be concluded, that the four modes of cyclization are possible, with a slight preference for the chair-like processes (**32**→**33**→**22** and **34**→**35**→**23**) over the twist-boat-like processes (**30**→**31**→**23** and **36**→**37**→**22**) yielding a 1:1 ratio of spiroacetals **22** and **23**.

It remains to examine the cyclization under kinetic control of the diastereoisomeric mixture of hydroxyenol ether **20** which gave a 3:2:5 ratio of spiroacetals **24**, **25**, and **26**. The racemic spiroacetals **24** and **25** arise from the cyclization of the (racemic) (2*RS*,2′*RS*)-diastereoisomer of **20**. Upon protonation, (2*RS*,2′*RS*)-**20** will give an oxocarbonium ion equivalent to **38a** (or **29a**) which can cyclize either *via* a twist-boat mode or a chair-like mode; the later would predominante over the former *via* an early transition state and thus explain the observed 3:2 ratio of **24**/**25**.

The amount of racemic spiroacetal **26** in mixtures obtained under both kinetic and thermodynamic control can be easily rationalized from the fact that in this case, only one such racemic product might be obtained from the cyclization of racemic diastereoisomeric (2*RS*,2′*SR*)-**20**. Indeed, cyclization of enantiomer (2*R*,2′*S*)-**20** on one face of the ring yields the enantiomer (2*R*,8*S*)-**26**, while the cyclization on the other side provides

(2*S*,8*R*)-**26**. In the light of the preceding discussion, one of these enantiomers of **26** must be formed preferentially over the other. But of course, the isolated **26** is totally racemic because the starting hydroxyenol ether (2*RS*,2′*SR*)-**20** was racemic.

It is now pertinent to reanalyze the previously reported mild-acid cyclization of bicyclic hydroxypropyl acetal **52** [8] [9] (*Scheme 6*). At room temperature, **52** gave only the *cis-transoid-trans*-tricyclic acetal **56** upon acid treatment (TsOH, MeOH; kinetic control). An equilibrium mixture of *cis*- and *trans-transoid-trans*-acetals **56** and **59** (45:55) was obtained only after refluxing under the same conditions (thermodynamic control). The cyclization under kinetic control to **56** was explained by the formation of oxocarbonium ion **53** which, under stereoelectronic control, gives either the *cis-transoid-trans*-acetal **56** *via* a chair-like pathway (→**54**→**55**) or the *trans-transoid-trans*-acetal **59** *via* a twist-boat pathway (→**57**→**58**). Since, the formation of **56** was exclusive, it was believed [8] that the transition state must be late resembling **55** rather than the less stable **58**. Nevertheless, in the light of the preceding results and other experimental evidence [6] [7] [10], it is unlikely that the exclusive formation of **56** arises from a late transition state. Interestingly, it is relatively easy, however, to understand the exclusive formation of *cis-transoid-trans*-acetal **56** *via* an early transition state *provided that there is a proper alignment of the incoming OH group with the p orbital of the oxocarbonium ion.* This stereoelectronic parameter corresponds approximately to the *Bürgi-Dunitz* angle of attack of a nucleophile on a π system [11]. This alignment is readily achieved in **54** but not in **57**. Modeling studies on oxocarbonium species **53** also support this argument.

Scheme 6. *Antiperiplanar-* vs. *Synperiplanar-Lone Pairs Hypothesis*

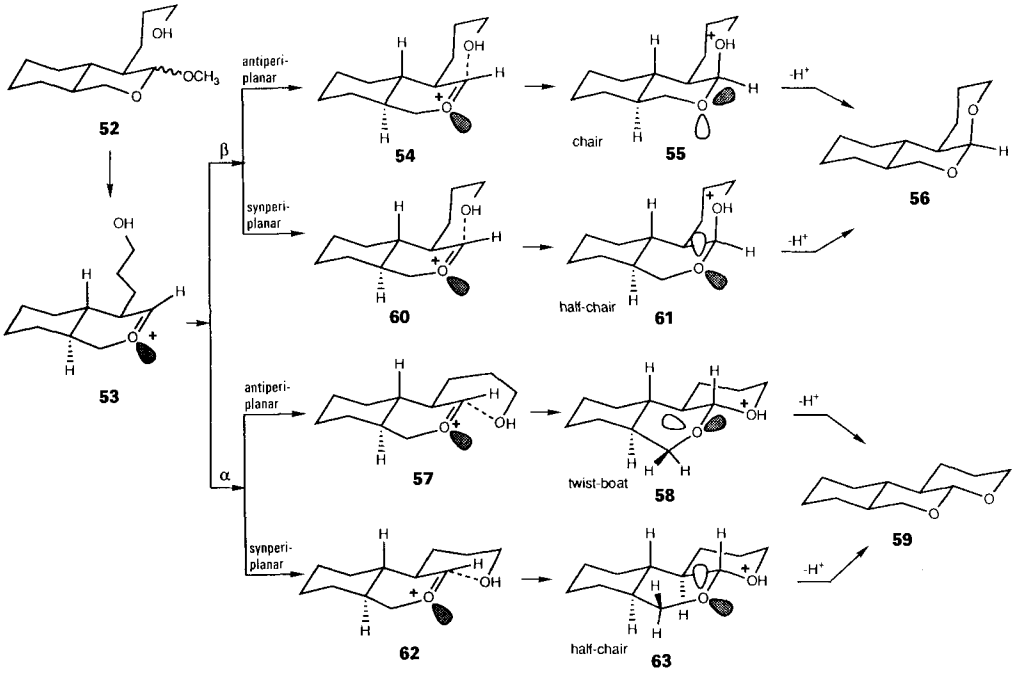

Indeed a conformational analysis[2]) (30° steps) on all exocyclic bonds of MINDO-3[3]) minimized **53** shows that the vast majority of the 1103 allowed conformers has the OH above the plane of the oxocarbonium ion (like in **54**) rather than underneath that plane (like in **57**). The distance from the hydroxyl O-atom to the oxocarbonium C-atom covers a range between 2.63 to 6.33 Å (0.1 Å grid). An examination of those conformers having shortest distances should give an indication about the easiest path of approach between the two reactive centers. *Table 2*

Table 2. *Representative* **54**-*Like and* **57**-*Like Conformers of Oxocarbonium Ion* **53**

	Entry	Distance [Å] O···C=O	Angle [°] O···C=O	Heat of formation [kcal/mol]
54-like	*1*	2.65	106	50
	2	2.75	103	51
	3	2.85	101	51
	4	2.85	111	49
	5	2.95	101	51
57-like	*6*	2.75	142	54
	7	2.95	144	55
	8	3.15	152	50
	9	3.25	148	50
	10	3.35	146	48

lists salient parameters for representative lowest-energy conformers of both types, *i.e.* **54**-like and **57**-like conformers, together with their heat of formation obtained from MINDO-3 semi-empirical calculations. The **54**-like and **57**-like lowest-energy conformer are also shown in the *Figure*. It is easily observed that the shortest O···C=O distance (2.65 Å) is obtained for a **54**-like conformer (*Entry 1*, O···C=O angle 106°, heat of formation 50 kcal/mol). The lowest-energy **54**-like conformer (*Entry 4*) has an O···C=O distance of 2.85 Å, and an O···C=O angle of 111°. Shortest O···C=O distances in **57**-like conformers are obtained at 2.75 Å and 2.95 Å. However, in these cases, heats of formation are *ca.* 3 to 4 kcal/mol higher than in the corresponding **54**-like conformers (*cf. Entries 2* and *6*, *5* and 7). The lowest-energy conformer (*Entry 10*) has an O···C=O distance of 3.35 Å. Another point of interest is the fact that whereas O···C=O angles of 101–111° may be readily achieved in **54**-like conformers, this is not the case for **57**-like conformers where such angles are bigger than 142°. Therefore, since **54**-like conformers have shortest O···C=O distances, lower energies, and *Bürgi-Dunitz* O···C=O angles, this approach path of the nucleophile (OH) should be preferred over the one starting from a **57**-like conformers.

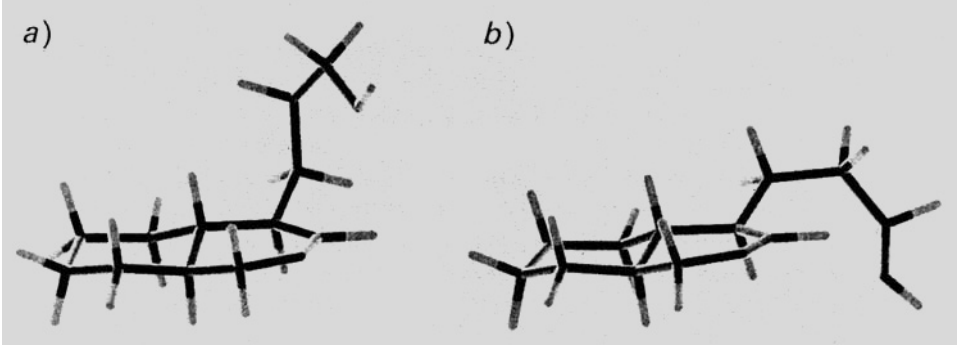

Figure. *Lowest-energy* a) **54**-*like and* b) **57**-*like conformers of oxocarbonium ion* **53** (see *Table 2*)

[2]) Conformational analysis was performed using the search (rigid rotor) module within SYBYL molecular-modeling software.

[3]) MINDO-3 Calculations (performed using the MOPAC package within SYBYL), are known to perform extremely well on carbonium ions giving heats of formation in excellent agreement with experimental results and *ab initio* calculations [12]. Structure **53** was constructed using SYBYL software. The hydroxypropyl chain was set in all staggered conformation following optimization of all bond lengths, valence and torsion angles.

In conclusion, an early-transition-state situation readily explains the exclusive formation of *cis-transoid-trans*-acetal **56**, as it explains nicely the 1:1 ratio of spiroacetals **22** and **23** from **18**. Furthermore, it also provides a simple explanation for the same 3:2 product ratio obtained in the cyclizations under kinetic control of **19** (→**22**/**23** 3:2), **20** (→**24**/**25** 3:2), and **21** (→**27**/**28** 3:2).

Fraser-Reid and colaborators [13] recently proposed that the hydrolysis (or formation) of glycosides could take place in some cases by a synperiplanar rather than an antiperiplanar lone pair pathway. Another pathway which is based on the principle of least motion but completely ignores stereoelectronic principle was also strongly advocated by *Sinnott* [14] in recent years. We will now examine these two alternative pathways and compare them with our hypothesis of an early-transition-state, antiperiplanar-lone-pair pathway for the cyclizations to acetals discussed above.

Taking the bicyclic hydroxyacetal **52** as an example, the synperiplanar-lone-pair hypothesis means that the cyclization of **53** could take place *via* a β-attack leading to a half-chair (→**60**→**61**) in order to give *cis-transoid-trans* acetal **56** or *via* an α-attack leading to a half-chair (→**62**→**63**) before giving *trans-transoid-trans*-acetal **59**. Now, if these reactions take place *via* a *very early* transition state, it can be seen that **54** and **60** on one hand and **57** and **62** on the other hand, respectively, are virtually identical! Kinetically, they are equivalent and there is no need to discuss further the antiperiplanar *vs.* the synperiplanar mechanisms on this basis. Consequently, it should be noted that the experimental results on *acetal cleavages* reported by *Fraser-Reid* and coworkers cannot be considered as evidence in favor of the synperiplanar hypothesis, because these processes take place *via* a *late transition state*. On that basis, and as previously discussed in this paper, these results are equally well explained by the antiperiplanar hypothesis.

The structure of the transition state for the spontaneous hydrolysis of axial tetrahydropyranosyl acetals has been estimated from experimental structural and kinetic data by *Bürgi* and *Dubler-Steudle* [15a]. This analysis indicates a late transition state. It follows from this work that the transition state for the proton-catalyzed cleavage must also be late, it must, therefore, be early for the reverse process which is consistent with the results given in the present work. Very recently, *Andrews, Fraser-Reid,* and *Bowen* [15b] have carried out an *ab initio* study of transition states in glycoside hydrolysis based on axial and equatorial 2-methoxytetrahydropyrans. This theoretical work also indicates that acetal hydrolysis takes place *via* a late transition state. Indeed, for the protonated axial anomer (α-glycoside), cleavage occurs *via* a half-chair transition state which gives a half-chair oxocarbonium ion. In the case of the protonated equatorial anomer (β-glycoside), cleavage takes place *via* an ^4E-endo sofa transition state and thence to oxocarbonium ion having the same geometry. It should be pointed out that the half-chair and the sofa oxocarbonium ions have a very close geometry and similar energy, the half-chair being slightly more stable (0.15 kcal/mol).

The next question which can be asked, however, concerns what happens just after the transition state, which pathway is preferred? Is the chair pathway **54**→**55** preferred over the half-chair pathway **60**→**61** in the formation of *cis-transoid-trans*-acetal **56**? Similarly, is the *trans-transoid*-acetal **59** more easily produced *via* the twist-boat (**57**→**58**) than *via* the half-chair pathway (**62**→**63**)? These questions are important, especially when the reverse process which takes place *via* a late transition state is considered. Indeed, in the reverse process, it becomes pertinent to know precisely which conformational change occurs in compounds **56** and **59** prior to the cleavage step.

The antiperiplanar hypothesis has received support both theoretically [16] [17] and experimentally [3] [4] which indicates that electronically, it is a lower-energy pathway than the synperiplanar one. Consequently, it appears safe to conclude that the antiperiplanar process is normally favored over the synperiplanar, unless unusual steric effects would prevent the former over the latter. Thus, based on steric and electronic reasons, the chair process **54**→**55** would be preferred over the half-chair pathway **60**→**61** and **57**→**58** over **62**→**63**.

Keeping the same bicyclic hydroxyacetal **52** as an example, the pathway proposed by *Sinnott* [14] predicts that **53** would form **56** *via* the twist-boat process **64**→**65** (*Scheme 7*), whereas **59** would be formed from the chair pathway **66**→**67**, in complete opposition with the antiperiplanar hypothesis.

Scheme 7. *Principle of Least Motion Hypothesis*

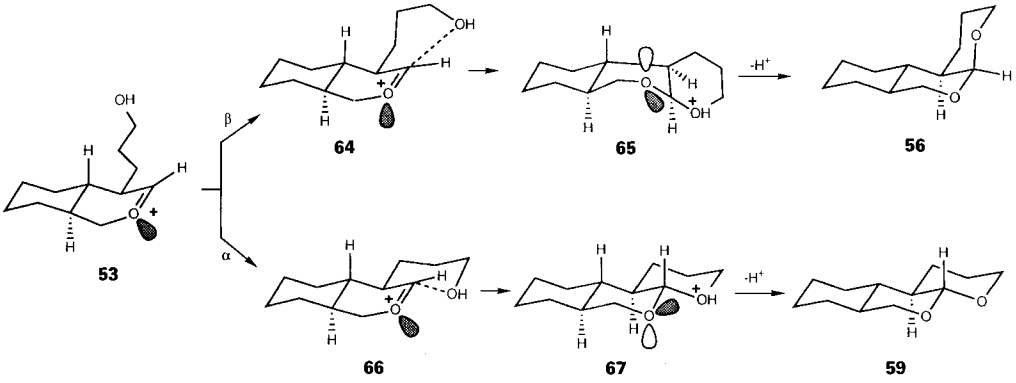

These conclusions were reached on the following basis: *1*) in pyridinio glycosides and due to a phenomenon called the reverse anomeric effect, the α-isomer is known to exist in the unusual twist-boat conformation **71** rather than in the usually more stable chair conformation **70**, whereas the β-isomer remains in the usual chair conformation **68** (*Scheme 8*). *2*) It was then postulated that the pyridinio β- and α-glycosides undergo hydrolysis directly from their ground state conformations **68** und **71**, respectively, to yield the corresponding oxocarbonium ion **72** by simply following the principle of least motion and postulating a late transition state, thus, completely neglecting the importance of stereoelectronics effects (or orbital overlap) during these processes.

On that basis, *Sinnott* concluded that the acid hydrolysis of α- and β-glycosides follows similar pathways because on protonation of the OR side chain, the β-glycosides would remain in the chair conformation **73** ($X = CH_3OH^+$), whereas the α-glycoside would change from the chair **75** to the twist-boat **76**. Then, the formation of the oxocarbonium ion **72** would come directly from **73** and **76** following the principle of least motion.

This hypothesis provides no driving force for the cleavage to take place, and we are convinced that it is false on the following basis: *1*) Following this hypothesis, the formation of **59** from the oxocarbonium ion **53** (→**66**→**67**) should proceed with equal ease as that of **56** (→**64**→**65**) under kinetically controlled conditions (*Scheme 7*), and hence the specific formation of **56** cannot be explained. *2*) Recent *ab initio* calculations

Scheme 8

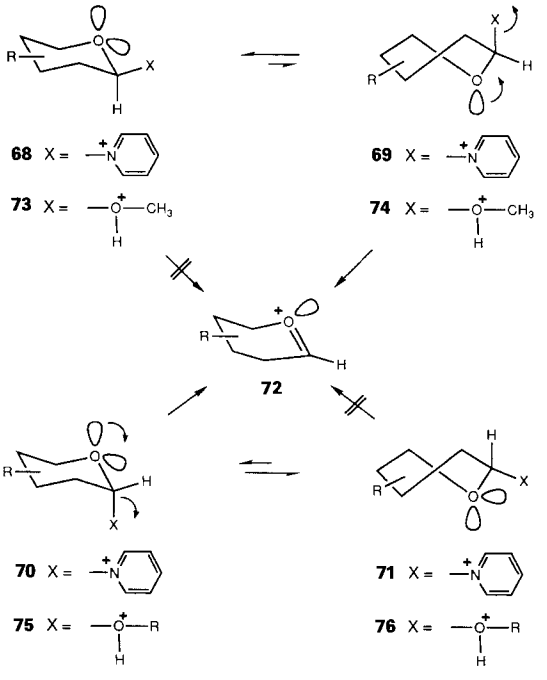

[17] on protonated species $H_nX{-}CH_2{-}Y^+H_n$ (X and Y = O and/or N) showed that, when a lone pair of X is antiperiplanar to the C–Y^+ bond, the C–X bond shortens, and the C–Y bond becomes much longer. In some cases, the tetrahedral species switch to a π-complex ($H_nX^+{=}CH_2 \cdots YH_n$). On the other hand, when one lone pair of X is *gauche* to the C–Y^+ bond, the C–Y^+ bond does not become longer. These calculations revealed also that tetrahedral intermediates having no antiperiplanar lone pairs are energetically quite stable species, indicating that the *reverse anomeric effect is a stabilizing electronic effect*. Furthermore, these calculations strongly suggest that the reverse anomeric effect is the result of an electrostatic attraction between the electron lone pairs of atom X and the positive charge of atom Y. Thus, in α-pyridinio glycosides, the twist-boat **71** is more stable than the chair conformation **70**, because the N^+ is *gauche* to the two lone pairs of the ring O-atom. In the case of the β-isomer, it stays in the same chair conformation, because the N^+ is already *gauche* to the two lone pairs of the ring O-atom.

On this basis, one can postulate that although β-pyridinio glycosides exist in the ground-state chair conformation **68**, they will then undergo a conformational change to the twist-boat **69** before reaching the transition state which will produce the oxocarbonium ion **72**. On the other hand, the α-pyridinio glycosides which exist in the ground-state twist-boat conformation will undergo a conformational change to the chair conformation **70** before reaching the transition state which will eventually produce the cyclic oxocarbonium ion **72**. The α- and β-glycosides would behave similarly. Upon protonation of the OR group, β-glycosides would remain in the chair conformation **73**, but would have to undergo a conformational change to the twist-boat **74** prior to reaching the

transition state required for the formation of the oxocarbonium ion **72**. On the other hand, upon protonation, the α-glycoside would undergo a conformational change from the chair **75** to the now more stable twist-boat **76**. However, **76** cannot undergo a cleavage with stereoelectronic control, and would, therefore, undergo a conformational change back to the chair **75** in order to eventually reach the transition state leading to the oxocarbonium ion **72**.

There are other well known organic reactions which are believed to proceed *via* a conformational change prior to cleavage in order to undergo stereoelectronically controlled processes. A very well known case is the reductive elimination of *trans*-1,2-dibromocyclohexane. This compound exists in the diequatorial conformation on the ground state, but it must undergo a conformational change to the less stable diaxial orientation in order to produce cyclohexene. Note that the formation of cyclohexene does not occur directly from the diequatorial conformer, although this would follow the principle of least motion! Similarly, in the reverse process, the addition of Br_2 to cyclohexene will produce first *trans*-1,2-dibromocyclohexane in the diaxial conformation.

Finally, it is well known that reaction at the anomeric center in α- and β-glycosides proceed in some cases with retention and in others with inversion of configuration. These reactions are explained on the basis of an S_N2 and an S_N1 process, respectively. When the displacement reaction takes place *via* an S_N1 mechanism, it is definitely a process with a very late transition state, very near the oxocarbonium ion which is a discrete species under these conditions. When the process takes place *via* an S_N2 mechanism, it is again a late-transition-state operation, but in this case, the attacking species is nucleophilic enough to start reacting before the S_N1 mechanism is completed. Recent studies by *Banait* and *Jencks* [18] on the reactivity of α-D-glucopyranosyl fluoride are in complete accord with this conclusion. The S_N2 displacement must, therefore, have a geometry at the transition state where C(1) and O–C(5) of the glycosides must be sp^2 hybridized. So, these processes are also controlled stereoelectronically at the transition-state level [19]. In other words, the theory of stereoelectronic control [3] does not represent 'an over interpretation of small and elusive least-motion effects' [14], but it predicts the stereochemistry of the overall process including the transition state, although it cannot pinpoint the position of the transition state along the reaction coordinate. The position of the transition state will of course vary depending on the nature of the substrate and the reaction conditions (nucleophilic, catalyst, *etc.*). This information can, however, be obtained experimentally in specific cases as shown in our work and that of others [6] [7] [10] [18] and can receive support from theoretical calculation [15–17].

This research was supported by the *Natural Sciences Engineering Research Council of Canada (NSERCC)* and by the 'Ministère de l'Éducation (*FCAR*)' of Québec. We acknowledge the *I.B.M. Canada Ltd. Company* (Cooperative Project Program) and the *Tripos Company* for support that allowed us to use the SYBYL software as well as Prof. *A. Michel* for helpfull discussions.

Experimental Part

General. All reactions, with the exception of catalytic hydrogenations, were executed under N_2 and were monitored by TLC. The intermediates were purified by flash chromatography [20] (FC; AcOEt/hexane, silica gel) and the final hydroxyenol ethers **18–21** were purified by FC (silica gel, 2% Et_3N in AcOEt/hexane). All compounds

described, including the final spiroacetals **22**–**28**, were obtained pure. Commercially available δ-valerolactone (**1**) was purchased from *Aldrich Chemical Company Inc.* and used without any further purification, 5-methyl-δ-valerolactone (**2**) was obtained by catalytic hydrogenation (see below) of 3,6-dihydro-6-methyl-2*H*-pyran-2-one [21], and *trans*-perhydro-1*H*-2-benzopyran-3-one (**3**) was prepared by a well known procedure: *Baeyer-Villiger* oxidation [22] of *trans*-hydrindanone [23]. IR Spectra: *Perkin-Elmer-681* spectrophotometer. ^{1}H- and ^{13}C-NMR Spectra: *Bruker-WM-250* spectrometer equipped with an *Aspect-2000* computer; at 250 MHz for ^{1}H and 63 MHz for ^{13}C; the free-induction decays (FID's) were sampled over 3000 Hz for ^{1}H and 10000 Hz for ^{13}C using 16384 data points; δ in ppm, J in Hz; ^{1}H: $CDCl_3$ or C_6D_6 (for **18**–**28**) solns., internal standard residual $CHCl_3$ (7.26 ppm) or residual C_6H_6 (7.15 ppm); ^{13}C: C_6D_6 solns. at 300 K for **18**–**28** and all cyclization experiments, solvent signal at 128.0 ppm as internal standard. MS: *Micromass-ZAB-1F* spectrometer.

*5-Methyl-δ-valerolactone (= 3,4,5,6-Tetrahydro-6-methyl-2*H*-pyran-2-one;* **2**). For 6 h, 3,6-dihydro-6-methyl-2*H*-pyran-2-one (39.2 g, 0.35 mol) was hydrogenated over PtO_2 at 40 psi in AcOEt (100 ml). Filtration and evaporation gave pure **2** (35 g, 87%) which was used without further purification. IR: 3000–2860, 1740, 1240, 1070. ^{1}H-NMR: 1.38 (*d*, J = 6.0 Me); 1.52 (*m*, $CH_2CH_2CH_2$); 1.90 (*m*, CH_2CH); 2.50 (*m*, CH_2C=O); 4.43 (*m*, CH–O).

*4-[(*tert*-Butyl)diphenylsilyloxy]but-1-yne* (**4**). To a stirred soln. of (*tert*-butyl)diphenylsilyl chloride (137.4 g, 0.5 mol) and imidazole (68 g, 1.0 mol) in CH_2Cl_2 (500 ml) at 0° in an ice-bath was added commercially available but-3-yn-1-ol (35 g, 0.5 mol). The mixture was stirred overnight at r.t. and then diluted to 1.5 l with CH_2Cl_2, the org. phase washed with H_2O (2 × 200 ml), 1N aq. HCl (2 × 200 ml), and 1N aq. $NaHCO_3$ (1 × 200 ml), dried ($MgSO_4$), and evaporated, and the residue distilled (125°/50 μ): 149 g (95%) of **4**. IR: 3300, 3070–2860, 1110. ^{1}H-NMR: 1.07 (*s*, *t*-Bu); 1.96 (*t*, J = 3.0, CH≡C); 2.46 (*td*, J = 6.6, 3.0, CH_2C≡C); 3.79 (*t*, J = 6.6, CH_2O); 7.40 (*m*, 6 H, H_m, H_p); 7.68 (*m*, 4 H, H_o).

*4-[(*tert*-Butyl)diphenylsilyloxy]pent-1-yne* (**5**). As described for **4**, from (*t*-Bu)Ph_2SiCl (137.4 g, 0.5 mol), imidazole (68 g, 1.0 mol), and commercially available (±)-pent-4-yn-2-ol (42 g, 0.5 mol). Distillation (125°/40 μ) gave 154 g (94%) of **5**. IR: 3310, 3080–2860, 1110. ^{1}H-NMR: 1.08 (*s*, *t*-Bu); 1.21 (*d*, J = 6.0, Me); 1.94 (*t*, J = 3.0, CH≡C); 2.32 (*m*, CH_2C≡C); 3.99 (*sext.*, J = 6.0, CH–O); 7.40 (*m*, 6 H, H_m, H_p); 7.69 (*m*, 4 H, H_o).

*9-[(*tert*-Butyl)diphenylsilyloxy]-1-hydroxydec-6-yn-5-one* (**6**). A soln. of **5** (8.05 g, 25 mmol) in anh.THF (50 ml) was stirred for 30 min at −78° (dry ice/acetone). Then 1.6M BuLi in hexanes (25 mmol, 15.6 ml) was added dropwise and the soln. stirred at −78° for further 90 min. A soln.of **1** (2.5 g, 25 mmol) in anh. THF (25 ml) was then added dropwise, slowly, and after addition, the mixture was stirred at −78° for 3 h. Then the mixture was quenched with H_2O (5 ml), allowed to warm to r.t., and diluted with Et_2O (200 ml).The org. phase was washed with 1N aq. $NaHCO_3$ (2 × 50 ml), dried ($MgSO_4$), and evaporated and the crude oil submitted to FC (AcOEt/hexane, silica gel): pure **6** (10.5 g, 99%). IR: 3400, 3100–2860, 2220, 1675, 1110. ^{1}H-NMR: 1.08 (*s*, *t*-Bu); 1.22 (*d*, J = 6.0, CH_3); 1.65 (*m*, CH_2CH_2); 2.48 (*t*, J = 6.0, CH_2C≡C); 2.55 (*t*, J = 6.0, CH_2C=O); 3.64 (*t*, J = 6.0, CH_2O); 4.04 (*sext.*, J = 6.0, CH–O); 7.40 (*m*, 6 H, H_m, H_p); 7.69 (*m*, 4 H, H_o).

*1-[(*tert*-Butyl)diphenylsilyloxy]-9-hydroxydec-3-yn-5-one* (**7**). As described for **6**, from **2** (4.56 g, 40 mmol) in THF (40 ml), **4** (12.32 g, 40 mmol) in THF (75 ml), and 1.6M BuLi in hexanes (40 mmol, 25.0 ml): 14.0 g (92%) of **7**. IR: 3440, 3100–2860, 2220, 1675, 1115. ^{1}H-NMR: 1.08 (*s*, *t*-Bu); 1.18 (*d*, J = 6.0, Me); 1.45 (*m*, CH_2CH); 1.74 (*m*, $CH_2CH_2CH_2$); 2.56 (*t*, J = 7.0, CH_2C=O); 2.62 (*t*, J = 7.0, CH_2C≡C); 3.77 (*sext.*, J = 6.0, CH–O); 3.82 (*t*, J = 7.0, CH_2O); 7.40 (*m*, 6 H, H_m, H_p); 7.68 (*m*, 4 H, H_o).

*2-[(*tert*-Butyl)diphenylsilyloxy]-10-hydroxydec-4-yn-6-one* (**8**). As described for **6**, from **2** (11.4 g, 0.1 mol) in THF (40 ml), **5** (32.2 g, 0.1 mol) in THF (100 ml), and 1.6M BuLi in hexanes (0.1 mol, 62.5 ml): 39.0 g (90%) of **8**. IR: 3400, 3080–2860, 2220, 1675, 1110. ^{1}H-NMR: 1.08 (*s*, *t*-Bu); 1.18 (*d*, J = 6.0, 3 H–C(11)); 1.22 (*d*, J = 6.0, 3 H–C(1)); 1.45 (*m*, CH_2CHOH); 1.73 (*m*, $CH_2CH_2CH_2$); 2.47 (*dd*, J = 6.0, 2.0, CH_2C≡C); 2.53 (*t*, J = 7.0, CH_2C=O); 3.77 (*sext.*, J = 6.0, CHOH); 4.03 (*sext.*, J = 6.0, CHOSi); 7.40 (*m*, 6 H, H_m, H_p); 7.69 (*m*, 4 H, H_o).

*6-[(*tert*-Butyl)diphenylsilyloxy]-1-[(*trans*-2-(hydroxymethyl)cyclohexyl]hex-3-yn-2-one* (**9**). As described for **6**, from **3** (1.54 g, 10 mmol) in THF (15 ml), **4** (3.12 g, 10 mmol) in THF (25 ml), and 1.6M BuLi in hexanes (10 mmol, 6.3 ml): 4.19 g (90%) of **9** and its hemiacetal. IR: 3370, 3080–2840, 2240, 2210, 1670, 1110. ^{1}H-NMR: 1.06 (*s*, 9 H, *t*-Bu, hemiacetal); 1.09 (*s*, 9 H, *t*-Bu, **9**); 1.80–0.75 (*m*, 20 H, 8 CH_2, 4 CH, **9** and hemiacetal); 1.95 (*m*, 2 H, CH_2COO, hemiacetal); 2.80–2.35 (*m*, 6 H, CH_2C≡C of **9** and hemiacetal, CH_2C=O of **9**); 3.85–3.40 (*m*, 8 H, CH_2OH and CH_2OSi of **9**, CH_2O and CH_2OSi of hemiacetal); 7.40 (*m*, 12 H, H_m, H_p, **9** and hemiacetal); 7.69 (*m*, 8 H, H_o, **9** and hemiacetal).

*9-[(*tert*-Butyl)diphenylsilyloxy]-1-hydroxydecan-5-one* (**10**). Hydrogenation of **6** (6.33 g, 15 mmol) over PtO_2 at 40 psi for 4 h in AcOEt (30 ml), filtration, evaporation, and FC (AcOEt/hexane, silica gel) of the resulting crude oil gave pure **10** (6.0 g, 94%). IR: 3410, 3080–2860, 1710, 1110. ^{1}H-NMR: 1.05 (*s*, *t*-Bu); 1.07 (*d*, J = 6.0, Me); 1.35–1.70 (*m*, 4 CH_2); 2.26 (*t*, J = 6.0, CH_2C=O); 2.38 (*t*, J = 6.0, CH_2C=O); 3.62 (*q*, J = 6.0, CH_2O); 3.83 (*sext.*, J = 6.0, CHOSi); 7.39 (*m*, 6 H, H_m, H_p); 7.67 (*m*, 4 H, H_o).

*1-[(*tert*-Butyl)diphenylsilyloxy]-9-hydroxydecan-5-one* (**11**). As described for **10**, from **7** (8.44 g, 20 mmol): 8.1 g (95%) of **11**. IR: 3420, 3080–2860, 1710, 1110. ^{1}H-NMR: 1.05 (*s*, *t*-Bu); 1.20 (*d*, *J* = 6.0, Me); 1.35–1.75 (*m*, 4 CH_2); 2.38 (*t*, *J* = 6.0, CH_2C=O); 2.43 (*t*, *J* = 6.0, CH_2C=O); 3.65 (*t*, *J* = 6.0, CH_2O); 3.76 (*m*, CH–O); 7.39 (*m*, 6 H, H_m, H_p); 7.68 (*m*, 4 H, H_o).

*2-[(*tert*-Butyl)diphenylsilyloxy]-10-hydroxydecan-6-one* (**12**). As described for **10**, from **8** (10.9 g, 25 mmol): 9.9 g (90%) of **12**. IR: 3410, 3080–2860, 1710, 1110. ^{1}H-NMR: 1.05 (*s*, *t*-Bu); 1.06 (*d*, *J* = 6.0, 3 H–C(1)); 1.20 (*d*, *J* = 6.0, 3 H–C(11)); 1.35–1.75 (*m*, 4 CH_2); 2.26 (*t*, *J* = 6.0, CH_2C=O); 2.38 (*t*, *J* = 6.0, CH_2C=O); 3.78 (*m*, C*H*OH); 3.83 (*sext.*, *J* = 6.0, C*H*OSi); 7.40 (*m*, 6 H, H_m, H_p); 7.69 (*m*, 4 H, H_o).

*6-[(*tert*-Butyl)diphenylsilyloxy]-1-[*trans*-2-(hydroxymethyl)cyclohexyl]hexan-2-one* (**13**). As described for **10**, from **9** (1.40 g, 3 mmol): 1.30 g (92%) of **13**. IR: 3400, 3080–2850, 1740, 1110. ^{1}H-NMR: 1.08 (*s*, *t*-Bu); 1.90–0.80 (*m*, 8 CH_2, 2 CH); 3.80–3.40 (*m*, CH_2OH, CH_2OSi); 7.40 (*m*, 6 H, H_m, H_p); 7.68 (*m*, 4 H, H_o).

*6-{4-[(*tert*-Butyl)diphenylsilyloxy]pentyl}-3,4-dihydro-2*H*-pyran* (**14**). From a soln. of **10** (4.26 g, 10 mmol) and TsOH (32 mg) in dry benzene (250 ml), 200 ml of benzene were distilled along with the H_2O (*Dean-Stark* separator). Then the mixture was cooled to r.t. and diluted to 100 ml with Et_2O and the org. phase washed with 1N aq. NaOH (2 × 20 ml), dried ($MgSO_4$), and evaporated. TLC gave yellowish but pure **14** (4.0 g, 98%; final purification after desilylation, see below). IR: 3060–2850, 1670, 1110. ^{1}H-NMR: 1.08 (*d*, *J* = 6.0, Me); 1.20 (*s*, *t*-Bu); 1.35–2.10 (*m*, 5 CH_2); 3.75 (*t*, *J* = 6.0, CH_2O); 3.93 (*sext.*, *J* = 6.0, CH–O); 4.43 (*t*, *J* = 3.0, C=CH); 7.26 (*m*, 6 H, H_m, H_p); 7.82 (*m*, 4 H, H_o).

*6-{4-[(*tert*-Butyl)diphenylsilyloxy]butyl}-3,4-dihydro-2-methyl-2*H*-pyran* (**15**). As described for **14**, from **11** (4.26 g, 10 mmol): 3.88 g (95%) of **15**. IR: 3060–2850, 1670, 1110. ^{1}H-NMR: 1.15 (*d*, *J* = 6.0, Me); 1.18 (*s*, *t*-Bu); 1.25–1.95 (*m*, 4 CH_2); 2.09 (*t*, *J* = 7.0, CH_2C=C); 3.68 (*t*, *J* = 6.0, CH_2O); 3.75 (*m*, CH–O); 4.47 (br. *s*, C=CH); 7.24 (*m*, 6 H, H_m, H_p); 7.80 *m*, 4 H, H_o).

*6-{4-[(*tert*-Butyl)diphenylsilyloxy]pentyl}-3,4-dihydro-2-methyl-2*H*-pyran* (**16**). As described for **14**, from **12** (8.8 g, 20 mmol): 7.8 g (93%) of **16**. IR: 3080–2860, 1675, 1110. ^{1}H-NMR: 1.05 (*d*, *J* = 6.0, CH_3CHOSi); 1.08 (*s*, *t*-Bu); 1.25 (*d*, *J* = 6.0, CH_3CHO); 1.35–2.10 (*m*, 5 CH_2); 3.85 (*m*, CH–O, CHOSi); 4.39 (br. *s*, C=CH); 7.37 (*m*, 6 H, H_m, H_p); 7.70 (*m*, 4 H, H_o).

*3-{4-[(*tert*-Butyl)diphenylsilyloxy]butyl}-*trans*-4a,5,6,7,8,8a-hexahydro-1*H*-2-benzopyran* (**17**). As described for **14**, from **13** (4.66 g, 10 mmol): 4.0 g (90%) of **17**. IR: 3060–2840, 1670, 1110. ^{1}H-NMR: 0.80–1.9 (*m*, 6 CH_2, 2 CH); 1.19 (*s*, *t*-Bu); 2.10 (*t*, *J* = 7.0, CH_2C=C); 3.46 (*t*, *J* = 12.0, H_{ax}–C(1)); 3.69 (*t*, *J* = 6.0, CH_2OSi); 3.85 (*dd*, *J* = 12.0, 3.5, H_{eq}–C(1)); 4.33 (br. *s*, C=CH); 7.25 (*m*, 6 H, H_m, H_p); 7.80 (*m*, 4 H, H_o).

*5-(3,4-Dihydro-2*H*-pyran-6-yl)pentan-2-ol* (**18**). To a stirred soln. of **14** (2.9 g, 7.1 mmol) in dry THF (30 ml) at r.t. were added Et_3N (1 ml) and 1M Bu_4NF in THF (9 ml, 9 mmol). Stirring was continued overnight. Then the mixture was diluted to 150 ml with Et_2O, the org. phase washed with 1N aq. NaOH (3 × 25 ml), dried ($MgSO_4$), and evaporated, and the crude oil submitted to FC (AcOEt/2% Et_3N/hexane, silica gel): pure **18** (725 mg, 60%). IR: 3360, 3000–2850, 1675, 1070. ^{1}H-NMR: 0.98 (*d*, *J* = 6.0, Me); 1.48 (*m*, 3 CH_2); 1.82 (*q*, *J* = 6.0, CH_2CH=C); 2.08 (*t*, *J* = 7.5, CH_2C=CH); 3.52 (*sext.*, *J* = 6.2, CH–O); 3.77 (*t*, *J* = 5.0, CH_2O); 4.47 (*t*, *J* = 3.7, C=CH).

*4-(3,4-Dihydro-2-methyl-2*H*-pyran-6-yl)butan-1-ol* (**19**). As described for **18**, from **15** (3.0 g, 7.3 mmol), THF (30 ml), Et_3N (1 ml), and 1M Bu_4NF in THF (9 ml, 9 mmol): 800 mg (65%) of **19**. IR: 3350, 3000–2860, 1675, 1075. ^{1}H-NMR: 1.14 (*d*, *J* = 7.0, Me); 1.25–1.95 (*m*, 4 CH_2); 2.07 (*t*, *J* = 7.5, CH_2C=C); 3.35 (*t*, *J* = 6.2, CH_2O); 3.75 (*m*, CH–O); 4.46 (br. *s*, C=CH).

*5-(3,4-Dihydro-2-methyl-2*H*-pyran-6-yl)pentan-2-ol* (**20**). As described for **18**, from **16** (3.42 g, 8.1 mmol), THF (30 ml), Et_3N (1 ml), and 1M Bu_4NF in THF (10 ml, 10 mmol): 1.04 g (70%) of **20**. IR: 3360, 3000–2840, 1675, 1100. ^{1}H-NMR: 0.99 (*d*, *J* = 6.0, 3 H–C(1)); 1.15 (*d*, *J* = 6.0, Me–C(2′)); 1.2–2.0 (*m*, 4 CH_2); 2.09 (*t*, *J* = 7.0, C=CCH_2); 3.53 (*sext.*, *J* = 6.0, C*H*OH); 3.77 (*m*, CH–O); 4.48 (br. *s*, C=CH).

*4-(*trans*-4a,5,6,7,8,8a-Hexahydro-1*H*-2-benzopyran-3-yl)butan-1-ol* (**21**). As described for **18**, from **17** (2.8 g, 6.0 mmol), THF (30 ml), Et_3N (1 ml), and 1M Bu_4NF in THF (8 ml, 8 mmol): 760 mg (60%) of **21**. IR: 3340, 3000–2850, 1665, 1050. ^{1}H-NMR: 0.65–1.70 (*m*, 6 CH_2, 2 CH); 2.10 (*t*, *J* = 7.0, C=CCH_2); 3.37 (*t*, *J* = 6.0, CH_2OH); 3.48 (*t*, *J* = 12.0, H_{ax}–C(1′)); 3.87 (*dd*, *J* = 12.0, 3.5, H_{eq}–C(1′)); 4.35 (br. *s*, C=CH).

Kinetically Controlled Cyclizations. All kinetically controlled cyclizations were conducted under the same conditions: The ^{13}C-NMR of hydroxyenol ether **18**, **19**, **20**, or **21** (1 mmol) in C_6D_6 (2.0 ml) was recorded at 300 K. Then, AcOH (1 mmol) was added and the cyclization followed by recording ^{13}C-NMR spectra at different times. After complete disappearance of the starting material, the data were collected, and the ratio of the spiroacetals was determined by integration of the signals of the O-bearing C-atoms (C(2) and C(8)). The mixture was then poured into 1N aq. NaOH, the aq. phase washed with Et_2O (3 × 20 ml), and the org. phase dried ($MgSO_4$) and evaporated. Purification of the spiroacetals was executed by FC (2% Et_3N/AcOEt/hexane, silica gel).

Thermodynamically Controlled Cyclizations. All thermodynamically controlled cyclizations were conducted under the same conditions as described above for the kinetically controlled cyclizations, except that CF_3COOH was used instead of AcOH reaction complete within 2 h.

Isomerizations. To the acetal mixture obtained from kinetically controlled cyclizations (**22**/**23** from **18** or **19**; **24**/**25**/**26** from **20**; **27**/**28** from **21**) was added CF_3COOH (3 drops).The ^{13}C-NMR spectrum was recorded after 2 h when equilibration was complete. Isolation and purification of the resulting acetal(s) followed the procedure used for the kinetically controlled cyclizations.

2-Methyl-1,7-dioxaspiro[5,5]undecanes **22** and **23** were obtained from **18** or **19** with AcOH in C_6D_6 (see kinetically controlled cyclization).

22: ^{1}H-NMR: 3.65 (*m*, CH_2O, CH–O); 2.1–1.2 (*m*, 6 CH_2); 1.15 (*d*, J = 6.0, Me).

23: ^{1}H-NMR: 4.18 (*ddd*, J = 12.0, 11.0, 2.0, H_{ax}–C(8)); 3.59 (*m*, H_{eq}–C(8)); 3.44 (*m*, H–C(2)); 1.95–1.05 (*m*, 6 CH_2); 1.20 (*d*, J = 6.0, Me).

2,8-Dimethyl-1,7-dioxaspiro[5.5]undecanes **24**–**26** were obtained from **20** with AcOH in C_6D_6 (see kinetically controlled cyclization).

24: ^{1}H-NMR: 3.70 (*m*, 2 CHO); 2.0–1.15 (*m*, 6 CH_2); 1.14 (*d*, J = 6.0, 2 Me).

25: ^{1}H-NMR: 3.80 (*m*, 2 CHO); 2.2–1.1 (*m*, 6 CH_2); 1.23 (*d*, J = 6.0, 2 Me).

26: ^{1}H-NMR: 4.13 (*m*, H–C(8)); 3.64 (*m*, H–C(2)); 2.2–1.1 (*m*, 6 CH_2); 1.22 (*d*, J = 6.0, Me–C(8)); 1.13 (*d*, J = 6.0, Me–C(2)).

Perhydrospiro [3H-benzopyran-3,2'-[2H]pyrans] **27** and **28** were obtained from **21** with AcOH in C_6D_6 (see kinetically controlled cyclization).

27: ^{1}H-NMR: 3.8–3.3 (*m*, 2 CH_2O); 2.1–0.7 (*m*, 8 CH_2 2 CH).

28: ^{1}H-NMR: 3.75–3.3 (*m*, 2 CH_2O); 2.2–0.7 (*m*, 8 CH_2, 2 CH).

REFERENCES

[1] P. Deslongchamps, D.D. Rowan, N. Pothier, G. Sauve, J.K. Saunders, *Can. J. Chem.* **1981,** *59,* 1105.

[2] P. Deslongchamps, N. Pothier, *Can. J. Chem.* **1987,** *68,* 597.

[3] P. Deslongchamps, 'Stereoelectronic Effects in Organic Chemistry', 'Organic Chemistry Series', Ed. J.E. Baldwin, Pergamon Press, Oxford, 1989, Vol. 1.

[4] a) A.J. Kirby, 'The Anomeric Effect and Related Stereoelectronic Effects at Oxygen', Springer-Verlag, Berlin, 1983; b) A.J. Kirby, *CRC Crit. Rev. Biochem.* **1987,** *22,* 283.

[5] a) P. Deslongchamps, D.D. Rowan, N. Pothier, J.K. Saunders, *Can. J. Chem.* **1981,** *59,* 1122; b) H. Beierbeck, J.K. Saunders, J.W. ApSimon, *ibid.* **1977,** *55,* 2813.

[6] P.R. Young, W.P. Jencks, *J. Am. Chem. Soc.* **1977,** *99,* 8238.

[7] R.A. McClelland, M. Ahmad, *J. Am. Chem. Soc.* **1978,** *100,* 7031.

[8] N. Beaulieu, R.A. Dickinson, P. Deslongchamps, *Can. J. Chem.* **1980,** *58,* 2531.

[9] P. Deslongchamps, D. Guay, *Can. J. Chem.* **1985,** *63,* 2757.

[10] A.J. Bennett, M.L. Sinnott, *J. Am. Chem. Soc.* **1986,** *108,* 7287.

[11] a) H.B. Bürgi, J.D. Dunitz, E. Shefter, *J. Am. Chem. Soc.* **1973,** *95,* 5065; b) H.B. Bürgi, J.D. Dunitz, *Acc. Chem. Res.* **1983,** *16,* 153.

[12] a) H.J. Koehler, H. Lischka, *J. Am. Chem. Soc.* **1979,** *101,* 3479; b) J. Chandrasekhar, P.v.R. Schleyer, H.B. Schlegel, *Tetrahedron Lett.* **1978,** 3393; c) P.v.R. Schleyer, J. Chandrasekhar, *J. Org. Chem.* **1981,** *46,* 225; d) A.C. Hopkinson, I.G. Csizmadia, *Can. J. Chem.* **1974,** *52,* 546.

[13] A.J. Ratcliffe, D.R. Mootoo, C.W. Andrews, B. Fraser-Reid, *J. Am. Chem. Soc.* **1989,** *111,* 7661.

[14] M.L. Sinnott, *Chem. Rev.* **1990,** *90,* 1171, and ref. cit. therein.

[15] a) H.B. Bürgi, K.C. Dubler-Steudle, *J. Am. Chem. Soc.* **1988,** *110,* 7291; b) C.W. Andrews, B. Fraser-Reid, J.P. Bowen, *J. Am. Chem. Soc.* **1991,** *113,* 8293.

[16] J.J. Irwin, T.K. Ha, J.D. Dunitz, *Helv. Chim. Acta* **1990,** *73,* 1805.

[17] a) F. Grein, P. Deslongchamps, *Can. J. Chem.*, in press; b) *ibid.*, in press.

[18] N.S. Banait, W.P. Jencks, *J. Am. Chem. Soc.* **1991,** *113,* 7951, 7958.

[19] J.A. Berson, *Acc. Chem. Res.* **1991,** *24,* 215.

[20] W.C. Still, M. Kahn, A. Mitra, *J. Org. Chem.* **1978,** *43,* 2923.

[21] D.T. Belmont, L.A. Paquette, *J. Org. Chem.* **1985,** *50,* 4102.

[22] J. Meinwald, E. Fravenglass, *J. Am. Chem. Soc.* **1960,** *82,* 5235.

[23] a) G.A. Haggis, L.N. Owen, *J. Chem. Soc.* **1953,** 389; b) E. Ali, L.N. Owen, *ibid.* **1985,** 2111; c) W. Hückel, W. Egerer, *Ann. Chem.* **1961,** *645,* 162.